VTL-PUB-49
(JANUARY 1978)

Preprint # 30,579

#338

MULTIPLICITY DISTRIBUTIONS AND DOUBLE-SCATTERING EFFECTS IN $\pi^- d$ INTERACTIONS AT 360 GeV/c*

K. Moriyasu, T. Burnett, D. Holmgren, H.J. Lubatti, D. Rees, G. Swider, B. Yuldashev†

Visual Techniques Laboratory, Department of Physics
University of Washington, Seattle, Washington 98195

K. Dziunikowska, A. Eskreys, K. Eskreys, A. Gula, D. Kisielewska, H. Rudnicka††, P. Stopa

Institute of Nuclear Physics and Institute of Nuclear Physics and Technology of the Academy of Mining and Metallurgy
Kawiory 26A, 30-055 Krakow, Poland

W. Ko, R.L. Lander, J.S. Pearson, D. Pellett, P. Yager

Department of Physics, University of California
Davis, California 95616

H. Abramowicz, M. Bardadin-Otwinowska, R. Gokieli, G. Sinapius, M. Szeptycka, A. Wroblewski, A. Zieminski

University of Warsaw and Institute of Nuclear Research
Hoza 69, 00-681 Warsaw, Poland

* Work supported in part by the National Science Foundation

† Visitor from Physical Technical Institute, Uzbek Academy of Sciences, Tashkent 700052, USSR.

†† Presently at the Visual Techniques Laboratory, Department of Physics, University of Washington, Seattle, Washington 98195.

ABSTRACT:

Double-scattering effects are studied in $\pi^- d$ interactions at 360 GeV/c. The partial cross sections $\sigma_N(\pi^- d)$, $\sigma_N(\text{"}\pi^- p\text{"})$ and $\sigma_N(\text{"}\pi^- n\text{"})$ are presented. The double-scattering probability per πd collision is found to be $f = 0.15 \pm 0.02$. We have extracted the partial cross section X_N of the double-scattering plus interference contributions, and find that X_N obeys KNO scaling. The data are compared with various theoretical predictions.

FERMILAB
FEB -3 1978
LIBRARY

1. INTRODUCTION

High energy scattering of hadrons on deuterons is of great interest in strong interaction physics. Double-scattering collisions, in which the incident hadron interacts with both the neutron and proton in the deuteron, provide a new and unique means of studying the space-time development of the strong interactions. In this regard, the deuteron target has particular advantages over heavier nuclei. Because of the loose binding and relatively large separation of the neutron and proton, the identification and interpretation of the double-scattering effects are essentially free of the complications encountered with heavier nuclei.

In this paper, we extend our previous study of double scattering in π^-d interactions (1,2,3) to a new energy of 360 GeV, the highest presently available at Fermilab. We examine the double-scattering effects in the multiplicity distribution and compare them to results at 205 GeV (1) and to recent theoretical predictions.

2. EXPERIMENTAL DETAILS

The data were obtained from a 52,000-picture exposure of the Fermilab 30-inch deuterium-filled bubble chamber to an unseparated 360 GeV negative-particle beam. The muon contamination in the beam was (1.0 ± 0.6)% as determined by Firestone et al. (4).

The pictures were scanned twice for all beam interactions in a fiducial region 36.7 cm long. Any discrepancies between the two scans were resolved by a third scan. All primary interactions, electron-positron pairs, and neutral strange particles were recorded. The number of incoming beam tracks was counted in all scannable pictures, and the total number of outgoing tracks was counted for each primary interaction. All short recoil tracks

and highly ionizing positive tracks were recorded as potential spectator protons or deuterons, and these tracks were measured in order to identify the true spectator protons. The minimum recoil momentum which is detectable is ∿ 80 MeV/c.†

A total of 9785 primary interactions were found with three or more charged secondary tracks ($N_{ch} \geq 3$). The one- and two-prong events have been omitted from our data sample due to the difficulty of correcting for π^-d coherent and π^-n elastic interactions. The scan efficiency for finding interactions with $N_{ch} \geq 3$ is essentially 100%.

3. MULTIPLICITY DISTRIBUTION

The multiplicity distribution of events for $N_{ch} \geq 3$ is presented in Table I and shown in Fig. 1, where we have applied corrections for Dalitz pairs, neutral strange particles decaying near the primary vertex, and electron pairs materializing near the vertex. The errors on the corrected multiplicity distribution include both the errors from the corrections and statistical errors. In addition the three- and four-prong events have been corrected for the substantial contributions from coherent interactions on the deuteron. We have used the coherent cross sections from π^-d data at lower energy (5) and subtracted them from our corrected three- and four-

---

† We have studied the effects of possible biases in the scanning of short tracks due to: (1) obscuring of short recoils by other produced tracks, (2) misidentification of δ-rays near the vertex as short spectators. We imposed cuts on the minimum proton momentum detectable and within statistics find no significant effects on any of our conclusions.

prong events.† The total corrected cross section determined for $N_{ch} \geq 3$ is 34.89 ± 0.47 mb, which corresponds to 3.65 μb/event.

The average number of produced negative particles, $< N_- >$, and the dispersion $D_- = \sqrt{< N_-^2 > - < N_- >^2}$, determined for $N_{ch} \geq 3$ are presented in Table II.†† The corresponding values for $\pi^- d$ data at 205 GeV (1), and $\pi^- p$ data at 205 (7) and 360 GeV (4) are included for comparison. Both the N_- and D_- values for $\pi^- d$ data at 360 GeV are larger than those observed in $\pi^- p$ interactions at the same energy. However, the values of the ratio $< N_- >/D_-$ are the same for $\pi^- d$ and $\pi^- p$ collisions at the two energies.

Interactions on deuterons produce events in which both an odd and an even number of charged tracks are observed. The odd-prong events are interpreted as $\pi^- n$ interactions in which the spectator proton is left with too little momentum to produce a visible track in the bubble chamber.# The even-prong events are of the following three types: (i) $\pi^- p$ interactions with a spectator neutron, (ii) $\pi^- n$ interactions with a spectator proton that is observed in the bubble chamber, (iii) interactions involving both the proton and neutron, i.e. double scattering.

---

† We used σ_3 (3πd) = 0.380 ± 0.049 mb and σ_4 (3πd) = 0.386 ± 0.044 mb, which are consistent with the estimate of total coherent 3πd at 205 GeV (6).

†† Since the coherent three and four-prong cross sections are nearly equal (and small compared with the πd inelastic cross section), the parameters of the distributions given in Table II are affected by less than one standard deviation if the coherent events are not removed.

From Ref. (7) we estimate the upper limit for contamination from even-prong events with recoil momentum less than 80 MeV/c to be much less than 1%.

It is possible to obtain a clean sample of $\pi^- n$ interactions by removing events of type (ii) from the even prongs and adding them to the odd-prong events. Even-prong events with recoil protons which are backwards in the laboratory frame are unambiguous $\pi^- n$ interactions of type (ii). After multiplying these events for each multiplicity N by 2.17† to account for the $\pi^- n$ interactions with forward spectator protons, these events are subtracted from the even-prong sample and reassigned to the odd-prong sample with multiplicity N-1 to form the effective partial cross section $\sigma_N(\text{"}\pi^- n\text{"})$. The remaining even-multiplicity events of type (i) and type (iii), which are a mixture of $\pi^- p$ interactions and double-scattering events, give the effective partial cross sections $\sigma_N(\text{"}\pi^- p\text{"})$. The resulting effective partial cross sections, $\sigma_N(\text{"}\pi^- p\text{"})$ and $\sigma_N(\text{"}\pi^- n\text{"})$, are given in Table I and shown in Fig. 2.

4. DOUBLE SCATTERING

The "$\pi^- p$" sample contains all of the double-scattering interactions. A measure of the double scattering is given by the difference between the effective and free-nucleon cross sections. Thus, we define the quantity Δ for $N_{ch} \geq 3$

$$\Delta \equiv \sum_{N\geq 3} [\sigma_N(\text{"}\pi^- p\text{"}) - \sigma_N(\pi^- p)] + \sum_{N\geq 3} [\sigma_N(\pi^- n) - \sigma_N(\text{"}\pi^- n\text{"})].$$

We note that Δ can include a contribution from the interference between single and double-scattering amplitudes, which means that Δ cannot be related to the

---

† The factor 2.17 is obtained by averaging the invariant flux factor over the measured backward spectator momentum distribution (see Ref. (8)).

double-scattering amplitude in a model independent way. This point has not been made in previous studies of double scattering. We expect $\sigma_N(\pi^- n)$ to be larger than $\sigma_N(\text{"}\pi^- n\text{"})$ because the $\pi^- n$ interactions which rescatter are included in $\sigma_N(\text{"}\pi^- p\text{"})$.

We assume $\sum_{N\geq 3} \sigma_N(\pi^- p) = \sum_{N\geq 3} \sigma_N(\pi^- n)^{\dagger}$ and obtain

$$\Delta = \sum [\sigma_N(\text{"}\pi^- p\text{"}) - \sigma_N(\text{"}\pi^- n\text{"})] = 5.27 \pm 0.69 \text{ mb}.$$

We calculate the probability of double scattering per $\pi^- d$ collision from the ratio $f = \Delta / \sum_{N \geq 3} \sigma_N(\pi^- d)$ and obtain $f = 0.15 \pm 0.02$. This value is consistent with our previous result at 205 GeV (1), and with the $\pi^+ d$ data at 100 GeV (9) and lower energy $\pi^- d$ at 15 (3) and 21 GeV (2).

The effect of double scattering on the multiplicity distribution can be seen in the ratio

$$\alpha_N = \sigma_N(\text{"}\pi^- p\text{"})/\sigma_N(\pi^- p)$$

which is shown in Fig. 3. We have used the $\pi^- p$ data at 360 GeV from Firestone et al. (4). The general behavior of α_N is similar to that observed at 205 GeV. We note that α_N shows a clear increase with N and rises above 2; in fact, at the highest multiplicities the amount of double scattering is comparable to single scattering.

We can study the partial cross section of the non-single scattering terms in $\sigma_N(\text{"}\pi^- p\text{"})$ by subtracting the free-nucleon $\sigma_N(\pi^- p)$. We normalize the

---

† This assumption has been tested at 205 GeV. Using charge symmetry, we took $\pi^+ p$ data for $N \geq 4$ and an estimate of the contribution from $\pi^+ p \to \pi^+ \pi^+ n$ in order to calculate $\sum_{N\geq 3} \sigma_N(\pi^- n)$. We obtain $\sum_{N\geq 3} [\sigma_N(\pi^- p) - \sigma_N(\pi^- n)] = 0.32 \pm 0.16$ mb, which is small compared with the statistical error in Δ.

$\pi^- p$ data to our "$\pi^- n$" sample for $N \geq 3$ and define the excess X_N as

$$X_N \equiv \sigma_N(\text{"}\pi^- p\text{"}) - \sigma_N(\pi^- p)[\sum_{N\geq 3} \sigma_N(\text{"}\pi^- n\text{"}) / \sum_{N\geq 3} \sigma_N(\pi^- p)],$$

where $\sum_{N\geq 3} X_N = \Delta$. Under certain assumptions, the partial cross section X_N can be shown to be directly related to the double-scattering contribution (10); however, in general, X_N also can have contributions from interference between single- and double-scattering amplitudes.

The calculated X_N distribution is presented in Table III and shown in Fig. 4 for this experiment and 205 GeV $\pi^- d$. The average number of negative particles produced

$$\langle N_- \rangle_X \equiv \sum_{N_- \geq 1} N_- X_{N_-} \Big/ \sum_{N_- \geq 1} X_{N_-},$$

and the dispersion D_- are presented in Table II. In Fig. 5, we compare $\langle N_- \rangle_X$ with $\langle N_- \rangle_{\pi^- p}$ for $\pi^- p$ data at available incident momenta. As expected, the $\langle N_- \rangle_X$ are systematically larger than the $\langle N_- \rangle_{\pi^- p}$ at all energies. However, the ratio $D_-/\langle N_- \rangle_X$ is consistent with the value observed in πp interactions.

Since a constant value for $D/\langle N \rangle$ is a necessary condition for KNO scaling (11), this raises the interesting phenomenological question of whether KNO scaling is approximately preserved when large double-scattering effects are present. To investigate this question, we have plotted $\sigma_N(\text{"}\pi^- p\text{"})$ and X_N in Fig. 6 using the KNO scaling variables for $N \geq 4$. The $\pi^- p$ data at 360 GeV also are plotted for comparison. The shapes of the $\sigma_N(\text{"}\pi^- p\text{"})$, X_N and $\sigma_N(\pi^- p)$

distributions are remarkably similar. This suggests that the double-scattering and interference terms in X_N obey KNO scaling to the same extent as πp scattering. It also has been observed that the multiplicities from collisions on heavy nuclei (12) at high energies may be consistent with KNO scaling.

5. COMPARISON WITH THEORY

Several different theoretical interpretations have been proposed recently for double-scattering effects on deuterons. Dar et al. (13) have shown that their Collective Tube Model (CTM) can describe some detailed features of $\pi^- d$ data at 205 GeV. A more general approach has been developed by Baker, Lubatti, Rogers, and Weis (BLRW) (14) for calculating double-scattering effects and has been applied to $\pi^{\pm} d$ and pd data between 100 and 300 GeV. The physical ideas behind these two theoretical approaches are quite different.

The CTM assumes that the incident hadron interacts simultaneously with the proton and neutron, and that the interaction resembles a single-scattering collision at a CM energy $s \simeq 2(M_n + M_p)p_L$, where p_L is the incident momentum in the laboratory. Thus the double-scattering contribution in the CTM is given by $\sigma_N(\pi^- p)$ at twice the laboratory momentum. The effective partial cross section $\sigma_N(\text{"}\pi^- p\text{"})$ from the CTM is

$$\sigma_N(\text{"}\pi^- p\text{"}) = (1-P_2)\sigma_N^{\pi p}(p_L) + P_2\sigma_N^{\pi p}(2p_L)$$

where P_2 is the probability of interacting simultaneously with both nucleons. We used $P_2 = 0.21$ as determined by Dar et al.

The theoretical work of BLRW is not a model <u>per se</u>, but rather an application of the conventional picture of the space-time development of hadronic interactions and the AGK "cutting rules" (15) to double scattering in deuterium.

In this picture, the incident hadron dissociates into virtual constituents which individually interact with the nucleons in the target. The BLRW effective partial cross section is

$$\sigma_N(\text{"}\pi^- p\text{"}) = \sigma_N(\pi^- p) + 1/2\ \sigma_N(1) + \sigma_N(2)$$

where $\sigma_N(1)$ is the interference between single and double scattering and $\sigma_N(2)$ is the double-scattering contribution. The multiplicity distribution $\sigma_N(1)$ is expected to resemble single scattering. Thus, the double-scattering effects in our data allow us to study $\sigma_N(2)$ which provide new information about strong interactions which cannot be obtained with hydrogen targets.

A good test of the two models is to compare their predictions for α_N with our experimental data. The two theoretical approaches give

$$\alpha_N = (1 - P_2) + P_2\sigma_N^{\pi p}(2p_L)/\sigma_N^{\pi p}(p_L) \qquad \text{(CTM)}$$

$$\alpha_N = C + \sigma_N(2)/\sigma_N(\pi^- p) \qquad \text{(BLRW)}$$

where C is given by $C \simeq [\sigma(\text{"}\pi^- p\text{"})-\Delta]/\sigma(\pi^- p) = 0.76$.

The CTM prediction requires data for the partial cross sections at twice the incident beam energy, i.e., 720 GeV, which we have obtained by using a modified KNO distribution (16) given by

$$\frac{\sigma_N}{\sigma_{inel}}(\langle N \rangle - \alpha) = \phi\left(\frac{N - \alpha}{\langle N \rangle - \alpha}\right).$$

The scaling function ϕ is approximated by a polynomial fit to $\pi^- p$ data between 50 and 360 GeV. We have used this modified KNO approach because the scaling condition, $(\langle N \rangle - \alpha)/D = \text{const.}$, is in better agreement with the $\pi^- p$ data than the usual KNO condition $\langle N \rangle/D = \text{const.}$ A fit to $(\langle N \rangle - \alpha)$ versus

D yields $\alpha = 1.15$. Extrapolating the $\langle N \rangle$ versus P_{LAB} dependence to 720 GeV, we obtain $\langle N \rangle = 9.8$.

In BLRW, the calculation of the $\sigma_N(2)$ term for the prediction of α_N involves the convolution in N_-

$$\rho_{N_-}(2) = \sum_{i=0}^{N_-} \rho_i(P_L/2)\rho_{N_- - i}(P_L/2),$$

where $\rho_i = \sigma_i/\Sigma\sigma_i$ and $P_L/2$ is one-half of the incident beam momentum. Since there are no $\pi^- p$ data at exactly one-half of 360 GeV, the modified KNO approach discussed above was used to obtain the $\pi^- p$ data at 180 GeV. Following BLRW, the $\rho_{N_-}(2)$ distribution is normalized to $\sigma(2) = \Sigma\sigma_N(2) = 3.62$ mb.

The theoretical α_N are compared to the data in Fig. 3. The α_N of BLRW predicts a more rapid increase with N than the CTM values. Both theoretical α_N are consistent with the data at low N values ($N < 16$), but the prediction of BLRW appears to agree better at large N.

Another test of the two models is to compare their predictions for $\langle N_- \rangle_X$ with the experimental data at different energies. Using our definition of X_N, the theoretical $\langle N_- \rangle_X$ values have been calculated for the CTM and the BLRW approach.† The results are shown in Fig. 5. The BLRW predictions appear to agree better with the $\langle N_- \rangle_X$ values at high energy, but the data are consistent with either theory due to the large errors.

† For BLRW, we take $X_N = \sigma_N(1) + \sigma_N(2)$, where $\Sigma\sigma_N(1) = \Delta_{exp} - \sigma(2)$ and $\sigma_N(1)$ has the same distribution observed for $\pi^- p$ interactions.

We note that the difference in the $\langle N_- \rangle_X$ values of CTM and BLRW can be understood from the different energy dependence of the double-scattering terms. The double-scattering contribution in the CTM behaves like $\ln(2P_L) = \ln P_L + \ln 2$ while the convolution for $\alpha_N(2)$ in BLRW behaves like $2\ln(P_L/2) = 2\ln P_L - 2\ln 2$. Thus for sufficiently large P_L, the average multiplicity of BLRW will exceed the CTM value by an amount proportional to $\sim \ln P_L$.

6. CONCLUSIONS

We have extended the study of double scattering in $\pi^- d$ interactions to 360 GeV. The probability of double scattering per $\pi^- d$ collision is found to be $f = 0.15 \pm 0.02$. This value is consistent with previous results and indicates that f is essentially constant over a wide range of energies.

We have extracted the partial cross section X_N of the double-scattering plus interference contributions. The average number of negative particles produced, $\langle N_- \rangle_X$, is systematically larger than $\langle N_- \rangle$ for πp interactions at all energies. However, the ratio $D_-/\langle N_- \rangle_X$ is consistent with the πp value. The X_N distribution also obeys KNO scaling to the same extent as πp scattering.

The Collective Tube Model and the theory of BLRW are able to describe the double-scattering effects in our data. BLRW provide a better prediction for the increase of α_N at high multiplicities, but increased statistics are needed to clearly distinguish between the two theories.

ACKNOWLEDGMENT

We would like to thank the staffs of the 30-inch bubble chamber and neutrino laboratories at FNAL and our scanning and measuring staffs for their assistance.

REFERENCES

1. K. Dziunikowska et al., Phys. Lett. 61B (1976) 316.
2. R.E. Ansorge et al., Nucl. Phys. B109 (1976) 197.
3. F. Porter et al., Univ. of California, Berkeley, and Univ. of Washington, to be published; F. Porter, Multiplicity Distributions and Nuclear Effects in $\pi^- d$ Interactions at 15 GeV/c, Ph.D. Thesis, University of California, Berkeley, UC PPG/77/9/1 (1977).
4. A. Firestone et al., Phys. Rev. D14 (1976) 2902.
5. R. Harris et al., Diffractive Dissociation of Pions in $\pi^- d$ Interactions at 15 GeV/c, VTL-PUB-43 (1977), to be published in Physical Review D.
6. G. Sinapius, Ph.D. Thesis, Warsaw University (1977) (unpublished).
7. D. Ljung et al., Phys. Rev. D15 (1977) 3163.
8. J. Bartke, Acta Phys. Polon. B7 (1976) 723.
9. J.E.A. Lys et al., Phys. Rev. D15 (1977) 1857.
10. H.J. Lubatti, University of Washington Internal Note VTL-HEP-57 (1977).
11. Z. Koba, H.B. Nielsen and P. Olesen, Nucl. Phys. B40 (1972) 317.
12. J.R. Elliott et al., Phys. Rev. Lett. 34 (1975) 607; J.W. Martin et al., Nuovo Cimento 25A (1975) 447; V.G. Grishin et al., Sov. Jour. Nucl. Phys. 19 (1974) 697; S.A. Azimov et al., Nucl. Phys. B107 (1976) 45.
13. A. Dar and Tran Thanh Van, Phys. Lett. 65B (1976) 455.
14. M. Baker et al., Phys. Rev. Lett. 39 (1977) 375; M. Baker et al., Hadron Structure and High-energy Hadron-deuteron Collisions, VTL-PUB-40 (1977).
15. V. A. Abramovski, V.N. Gribov, and O.V. Kancheli, Yad. Fiz. 18 (1973) 595 (Sov. Jour. Nucl. Phys. 18 (1974) 308).
16. A. Wroblewski, Calculation of $\pi^- p$ Topologic Cross Sections as an Input for CTM and BLRW Models, University of Washington, Internal Note VEL-HEP-55 (1977).

TABLE I

CORRECTED EVENTS AND PARTIAL CROSS SECTIONS IN 360 GeV $\pi^- d$ INTERACTIONS

No. of Prongs	Events Found	Corrected Number	$\sigma_N(\pi^- d)$mb	$\sigma_N(\text{"}\pi^- p\text{"})$mb	$\sigma_N(\text{"}\pi^- n\text{"})$mb
3	390	288.5 ± 24.7	1.05 ± 0.09		1.82 ± 0.13
4	925	843.5 ± 34.0	3.08 ± 0.14	2.32 ± 0.16	
5	351	353.9 ± 19.8	1.29 ± 0.08		2.03 ± 0.12
6	1100	1120.7 ± 35.3	4.09 ± 0.15	3.36 ± 0.16	
7	442	452.5 ± 22.7	1.65 ± 0.09		2.65 ± 0.14
8	1257	1280.7 ± 39.2	4.68 ± 0.16	3.68 ± 0.19	
9	495	504.1 ± 24.9	1.84 ± 0.10		2.68 ± 0.14
10	1173	1180.3 ± 40.2	4.31 ± 0.17	3.47 ± 0.18	
11	393	388.6 ± 23.3	1.42 ± 0.09		2.08 ± 0.12
12	973	967.8 ± 39.6	3.54 ± 0.16	2.87 ± 0.17	
13	303	298.4 ± 21.3	1.09 ± 0.08		1.58 ± 0.11
14	678	658.3 ± 35.6	2.40 ± 0.14	1.92 ± 0.15	
15	183	172.6 ± 17.3	0.63 ± 0.06		0.83 ± 0.08
16	393	368.7 ± 28.4	1.35 ± 0.11	1.15 ± 0.11	
17	98	90.0 ± 12.8	0.33 ± 0.05		0.54 ± 0.07
18	236	222.5 ± 21.9	0.81 ± 0.08	0.60 ± 0.09	
19	73	71.5 ± 10.9	0.26 ± 0.04		0.35 ± 0.05
20	139	129.3 ± 16.8	0.47 ± 0.06	0.38 ± 0.07	
21	38	33.5 ± 8.1	0.12 ± 0.03		0.14 ± 0.03
22	70	62.1 ± 11.9	0.23 ± 0.04	0.21 ± 0.04	
23	14	11.1 ± 4.9	0.040 ± 0.018		0.067 ± 0.024
24	29	24.1 ± 7.4	0.088 ± 0.027	0.062 ± 0.032	
25	7	6.4 ± 3.3	0.023 ± 0.012		0.037 ± 0.017
26	13	11.3 ± 4.7	0.041 ± 0.017	0.027 ± 0.021	
27	1	$0.05^{+1.40}_{-0.05}$	$0.0002^{+0.005}_{-0.0002}$		$0.007^{+0.010}_{-0.007}$
28	7	6.3 ± 3.4	0.023 ± 0.012	0.016 ± 0.015	
29	1	$1.19^{+1.23}_{-1.19}$	$0.0043^{+0.0045}_{-0.0043}$		$0.0043^{+0.0045}_{-0.0043}$
30	3	2.4 ± 2.2	0.0088 ± 0.0082	0.0088 ± 0.0082	
TOTAL	9785	9550 ± 118	34.89 ± 0.47	20.08 ± 0.55	14.81 ± 0.41

TABLE II

AVERAGE NUMBER AND DISPERSION OF PRODUCED NEGATIVE PARTICLES

	$\langle N_- \rangle$	D_-
$\pi^- d$ 360 GeV	4.01 ± 0.03 [a]	2.17 ± 0.09
$\pi^- d$ 205 GeV (1)	3.46 ± 0.02	1.91 ± 0.04
$\pi^- p$ 360 GeV (4)	3.62 ± 0.02	2.02 ± 0.01
$\pi^- p$ 205 GeV (7)	3.26 ± 0.03	1.79 ± 0.01
X_N $\pi^- d$ 360 GeV	4.94 ± 0.23 [b]	2.21 ± 0.14
X_N $\pi^- d$ 205 GeV	4.03 ± 0.17	2.10 ± 0.11

a) This value changes to 3.95 if the coherent cross sections are not subtracted.

b) This value changes to 4.75 if the coherent cross sections are not subtracted.

TABLE III

X_N DISTRIBUTION FOR 360 GeV π^-d INTERACTIONS

No. of Prongs	X_N (mb)
4	$0.0^{+0.18}_{-0.0}$
6	0.76 ± 0.19
8	0.78 ± 0.21
10	0.94 ± 0.21
12	0.99 ± 0.19
14	0.71 ± 0.16
16	0.43 ± 0.12
18	0.22 ± 0.10
20	0.23 ± 0.07
22	0.15 ± 0.05
24	0.037 ± 0.032
26	$0.013^{+0.021}_{-0.013}$
28	$0.012^{+0.015}_{-0.012}$
30	$0.007^{+0.008}_{-0.007}$

FIGURE CAPTIONS

FIG. 1 : Partial cross section $\sigma_N(\pi^-d)$ for 360 GeV π^-d interactions.

FIG. 2 : Effective partial cross sections, $\sigma_N(\text{"}\pi^-p\text{"})$ and $\sigma_N(\text{"}\pi^-n\text{"})$, obtained from 360 GeV π^-d interactions.

FIG. 3 : Ratio α_N of the effective partial cross section $\sigma_N(\text{"}\pi^-p\text{"})$ and the free-nucleon partial cross section $\sigma_N(\pi^-p)$ (4) at 360 GeV. Also shown are the predictions of BLRW (14) and CTM (13).

FIG. 4 : Excess partial cross section X_N extracted from π^-d interactions at 360 GeV and 205 GeV (1) where X_N is defined in the text.

FIG. 5 : Average number of negative particles produced, $\langle N_- \rangle_X$, for the X_N partial cross section at 15 GeV (3), 21 GeV (2), and 205 GeV (1) and 360 GeV. The π^-p values are shown for comparison. Also shown are predictions of BLRW (14) and CTM (13).

FIG. 6 : Plot of $\langle N \rangle (\sigma_N/\sigma_{inel})$ versus $(N/\langle N \rangle)$ for $N \geq 3$ for: (1) $\sigma_N(\text{"}\pi^-p\text{"})$ at 360 GeV; (2) X_N at 360 GeV; (3) $\sigma_N(\pi^-p)$ at 360 GeV (4).

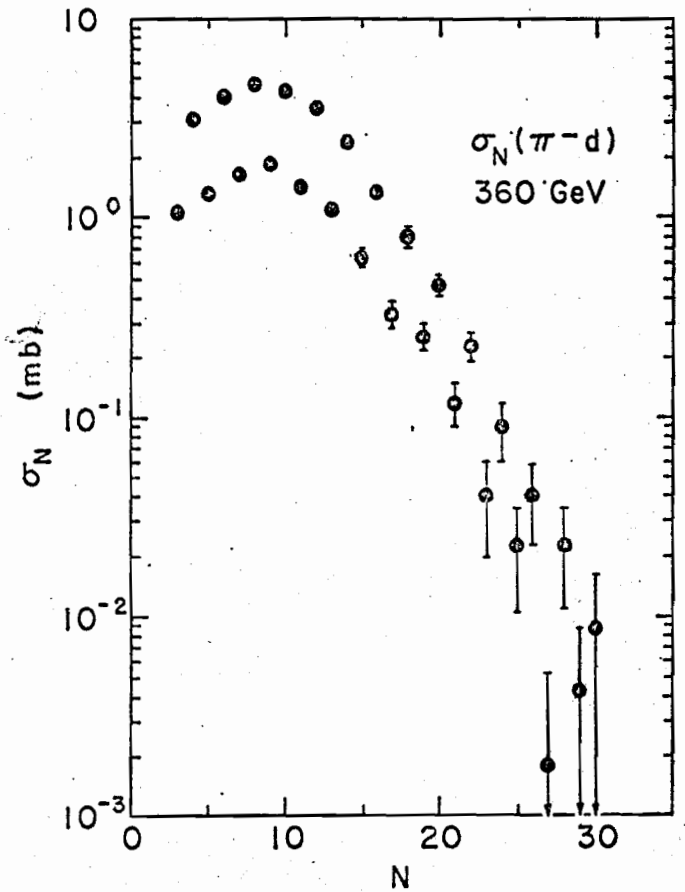
$\sigma_N(\pi - d)$
360 GeV
σ_N (mb)
N

FIG. 1

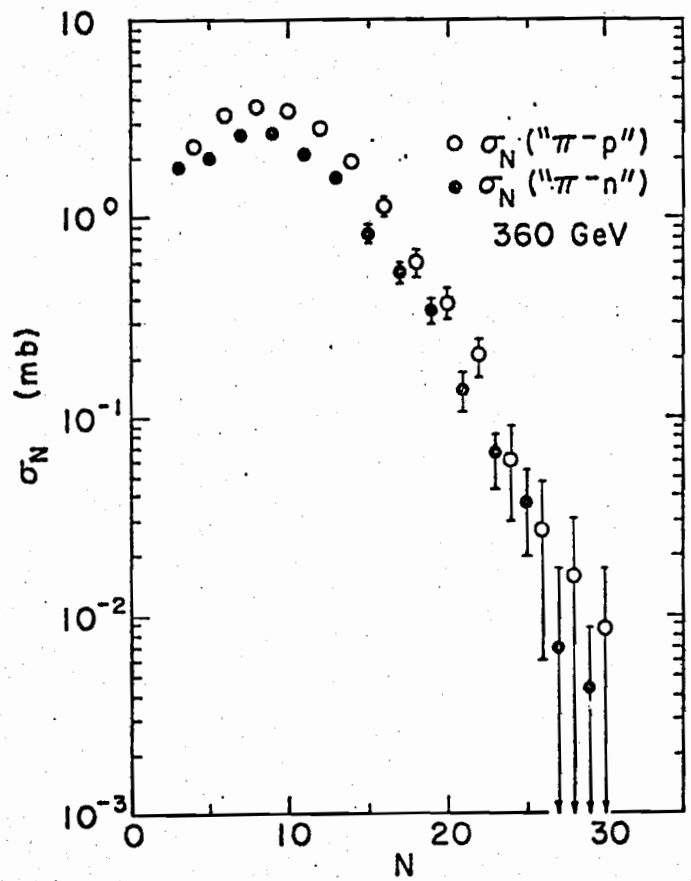
σ_N ("$\pi - p$")
σ_N ("$\pi - n$")
360 GeV
σ_N (mb)
N

FIG. 2

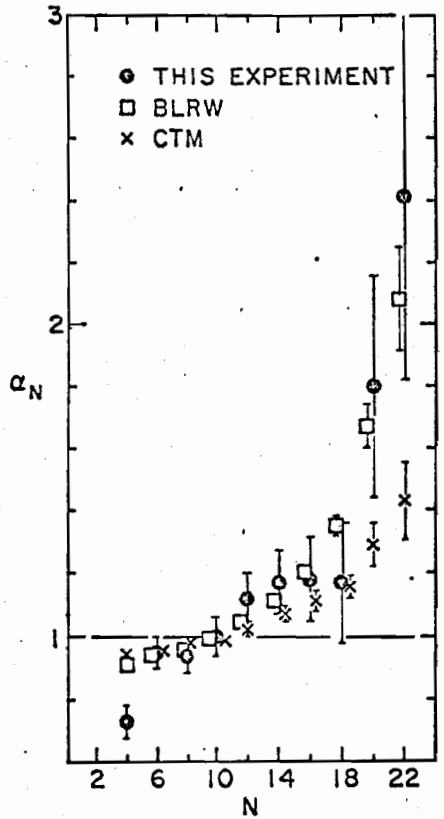
THIS EXPERIMENT
BLRW
CTM
α_N
N
3
2
1
2
6
10
14
18
22

FIG. 3

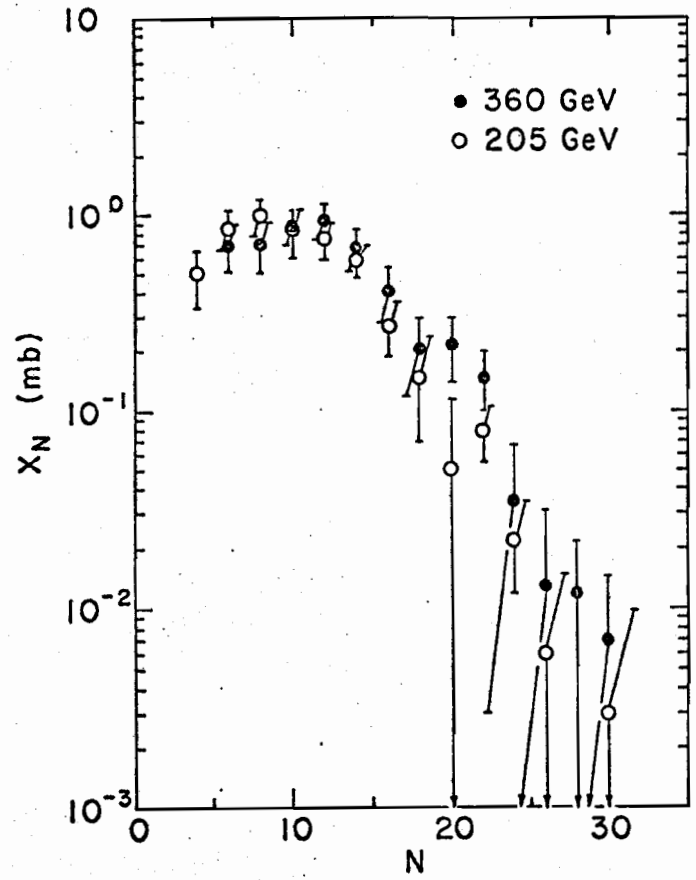
360 GeV
205 GeV
X_N (mb)
N
10
10^0
10^{-1}
10^{-2}
10^{-3}
0
10
20
30

FIG. 4

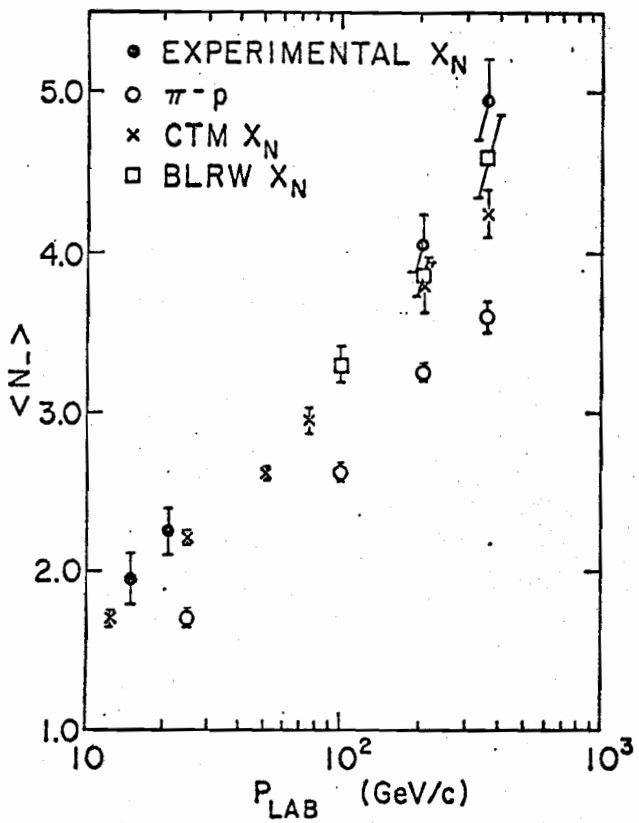
EXPERIMENTAL X_N
$\pi^- p$
CTM X_N
BLRW X_N
5.0
4.0
3.0
2.0
1.0
$\langle N_- \rangle$
10
10^2
10^3
P_{LAB} (GeV/c)

FIG. 5

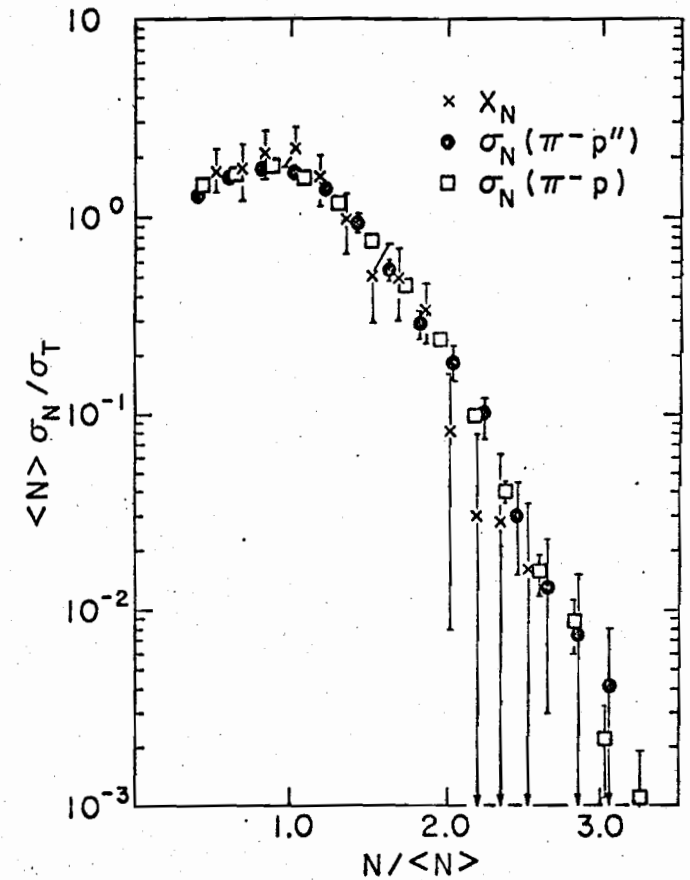
X_N
$\sigma_N(\pi^- p'')$
$\sigma_N(\pi^- p)$
10
10^0
10^{-1}
10^{-2}
10^{-3}
$\langle N \rangle \sigma_N / \sigma_T$
1.0
2.0
3.0
$N/\langle N \rangle$

FIG. 6